

High Degree of Optical Tunability of Self-Assembled Photonic-Plasmonic Crystals by Filling Fraction Modification

By Martín López-García, Juan F. Galisteo-López, Álvaro Blanco, Cefe López,* and Antonio García-Martín

The optical properties of two-dimensional hybrid photonic-plasmonic crystals are fine-tuned by modifying the dielectric component of the system. The filling fraction of the dielectric component in monolayers of spheres deposited on gold substrates is controlled by means of oxygen-plasma etching. Doing so enables spectral tuning of the optical modes of the system. Experiments are performed on both optically passive and active samples showing the possibility for strong modification of the emission properties of samples containing emitters distributed within the spheres. The change in sphere diameter needed to substantially modify the sample's optical response points to a potential use of these samples as sensors or tunable emitting devices if appropriate polymeric components are employed.

1. Introduction

Among the possible approaches to attain control over light propagation at the nano/microscale, plasmonic and photonic crystals have become two of the most powerful materials. Surface plasmon resonances (SPR) provide very large and localized field enhancement and integrability with microelectronics or supertransmission phenomena.^[1] On the other hand photonic crystals (PCs) have demonstrated novel routes for light control by means of density of states (DOS) engineering including full photonic bandgaps^[2] or strong modification of spontaneous emission in two- and three-dimensional (2D, 3D) systems.^[3,4] However, some intrinsic problems with these new structures have not yet been solved. On the one hand SPRs present very short propagation lengths, hampering their use in large-area devices. On the other hand organic PCs, attractive from the point of view of applications as well as for the ease and low cost of fabrication, lack the large refractive-index contrast needed

for experimentally realizing strong DOS modifications. A possible avenue to circumvent such limitations and obtain the best out of the above two systems would be their combined use in hybrid structures. Recent results have shown that coupling between waveguided modes associated with dielectric structures and plasmonic resonances may lead to laser devices on the nanoscale.^[5] Also exploiting hybrid plasmonic-photonic systems, SPR-supporting metallic structures can be loaded with structured organic materials. In this way, hybrid plasmonic-waveguided modes can be tailored to obtain large propagation lengths along with field enhance-

ments larger than those in their dielectric counterparts.^[6,7] A further step can be taken if the dielectric-metallic interface is modulated to achieve a PC structure. The latter system sustains modes propagating in the dielectric part that could be used, for instance, to obtain enhanced emission of internal sources.^[8,9] Among all the available techniques to obtain such a modulation in/over the metallic structure, self-assembly of monolayers of colloidal nanospheres is one of the most useful thanks to their large surface area,^[10] good crystalline quality and straightforward fabrication.^[11] Though typically used as templates for more complex structures in plasmonics^[12] the possibility of using these structures as PCs has also been demonstrated.^[13] Recently it has also been shown^[7,9,14–17] that when such PCs are grown over a SPR-supporting metallic film, hybrid photonic-plasmonic modes appear with strong field enhancement at different spatial positions in the sample.

The functionality of the above-described plasmonic-photonic systems could certainly be enhanced by changing their optical response under an external stimulus, turning them into tunable devices. Counted among the possible strategies are optical,^[18] electrical,^[19] magnetic^[20,21] or acoustic^[22] modifications of the plasmonic modes. Alternatively one can modify the refractive index or lattice constant of the organic lattice to tailor the photonic dispersion and hence the optical response of the system.^[23] Certain stimuli could even be employed to simultaneously tune both types of modes and the hybrid modes arising from them.

In this work we present an easy-to-implement processing method to tune the optical response of the hybrid modes of self-assembled monolayers of polymeric spheres deposited on

[*] M. López-García, Dr. J. F. Galisteo-López, Dr. Á. Blanco, Prof. C. López
Instituto de Ciencia de Materiales de Madrid (CSIC) and
Unidad Asociada CSIC-U. Vigo C/Sor Juana Inés de la Cruz 3
28049 Madrid, Spain
E-mail: cefe@icmm.csic.es
Dr. A. García-Martín
Instituto de Microelectrónica de Madrid (IMM-CSIC)
C/Iсаac Newton 8, 28760 Tres Cantos, Madrid, Spain

DOI: 10.1002/adfm.201001192

metallic films. For these systems, we have recently shown how the redistribution of the total field intensity can be exploited to strongly modify the spontaneous emission of internal sources.^[9] The tuning of their optical response is obtained by homogeneously reducing each sphere while keeping the lattice parameter constant, i.e. by changing the filling fraction of the hexagonal lattice as studied previously for PCs on dielectric substrates.^[24] In the present work we have used polystyrene (PS) spheres. Two diameters (0.52 and 1 μm) were tested for which the three kind of modes present in these systems, namely, waveguided-like (WG) plasmon-like (SPP) and hybrid modes, fall in the visible-NIR range.^[9] By means of oxygen-plasma etching each sphere in the monolayer is reduced in its entire volume in a controlled way while maintaining its lattice position. It is well known that isotropic oxygen-plasma etching constitutes an ideal method to reduce polymeric colloidal particles. This method has been used to modify the diameter of spheres forming monolayers on dielectric substrates^[25] as well as to locally change the filling fraction of 3D opal-based PCs to improve coupling to slow modes^[26] and to introduce planar defects.^[27] This fine-tuning was applied to close-packed monolayers deposited on thin gold films (60 nm). In this way the system modes can be modified in a controlled manner and experimentally monitored by means of VIS-NIR reflectance measurements. Experimentally observed blueshifts of the modes were measured and accounted for with numerical simulations. At the same time, the modification of the modal spatial profile was studied numerically in order to evaluate changes to field confinement within the structure. As a further step, the same process was applied to samples grown from dye-doped spheres for which enhanced emission at those frequencies matching the modes of the system has been previously reported.^[9] Emission spectra were collected after each etching step and it was found that changing the sample geometry upon etching strongly modifies the spontaneous emission of internal sources. The tuning process presented in this work is non-reversible and therefore suited for fine-tuning of the optical response of the system during the fabrication process. However, active devices based on the same principle could be obtained. Typical changes in diameter obtained (ca. 100 nm, i.e. 10% of sphere diameter) could be achieved with certain hydrogels as has been demonstrated already for 3D self-assembled structures. Hence, we believe the present method could be implemented in the future with similar materials, in order to develop a fully tunable emitting device in which changes over directionality or polarization can be attained.

2. Results and Discussion

Characterization prior to the etching process is required in order to estimate the filling fraction (ff) reduction of the lattice attained as a function of plasma time. Filling fraction is defined here as the ratio between the volume occupied by polystyrene divided by the volume of the unit cell of the lattice. Etching was performed on monolayers (sphere diameter $\phi = 1 \mu\text{m}$) for increasing plasma times. Scanning electron microscopy (SEM) was performed after each etching step in order to obtain each new sphere diameter. Two examples can be found in the insets

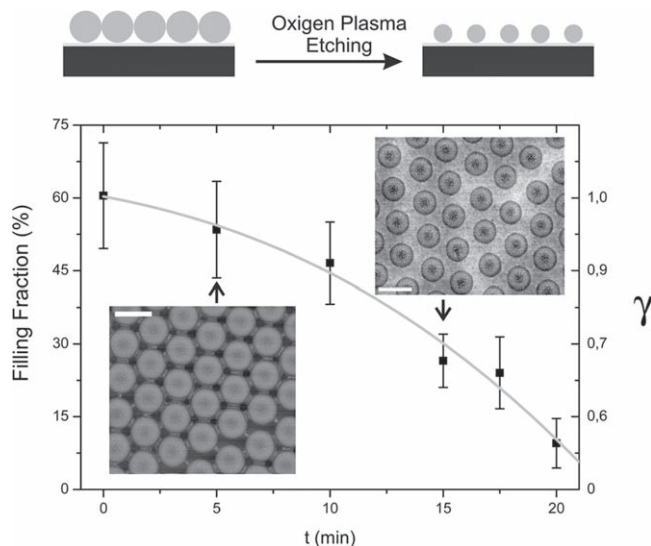


Figure 1. Plasma-etching reduction of initial diameter ($\Phi_0 = 1 \mu\text{m}$) PS spheres over a 20 minute period. Insets show SEM images for the same sample at two different etching times: 5 (bottom) and 15 (top) min. Scale bars correspond to 1 micron in both images. γ stands for the ratio between the final diameter (Φ_f) and the original Φ_0 one. The grey line fits to a third degree polynomial.

of **Figure 1**, corresponding to different points in the calibration graph. From the images it can be seen that, after each treatment, the sample retains a good crystalline quality and that the lattice parameter is larger than the diameter of the spheres. We can define a shrinkage parameter $\gamma = \frac{\phi_f}{\phi_0}$ to describe the etching. Thus we can express the filling fraction as $ff = \frac{\gamma^3 \pi}{3\sqrt{3}}$.

From the calibration plot of Figure 1 we can obtain the etching rate in this case for 1 μm diameter spheres. The reduction process is not a linear one, as would be expected from previous studies,^[28] and the fact that spheres in a close-packed configuration should be less affected by the plasma must be taken into account. That is, the etching ratio in the initial stages should be smaller than when the spheres have been appreciably shrunk. During the initial 10 minutes of etching in which we go from the close packed lattice ($ff = 0.60$ for the monolayer case) to a $ff = 0.44$, the reduction rate can be considered almost linear with a slow PS removing rate ($=\Delta\gamma = 0.01$ per minute) for 1 μm spheres. For longer treatments, PS etching is much faster. SEM images show that the crystalline quality of the lattice remains good during the first 15 minutes of etching time. For longer reduction times, spheres may lose their shape, making a more complex anisotropic etching technique necessary.^[25] Given that large diameter reductions are not the aim of this work (since optical quality can be severely damaged) we will concentrate on the initial slow linear reduction range. Though the amount of PS removed should be the same independent of sphere size, it is advisable that an etching calibration to obtain the ff reduction be performed for each sphere size studied. In our case a study was also carried out for the $\phi = 520 \text{ nm}$ spheres in the initial linear-like region.

In order to track the evolution of the optical response as homogenous sphere reduction takes place, normal reflectance

REFLECTANCE

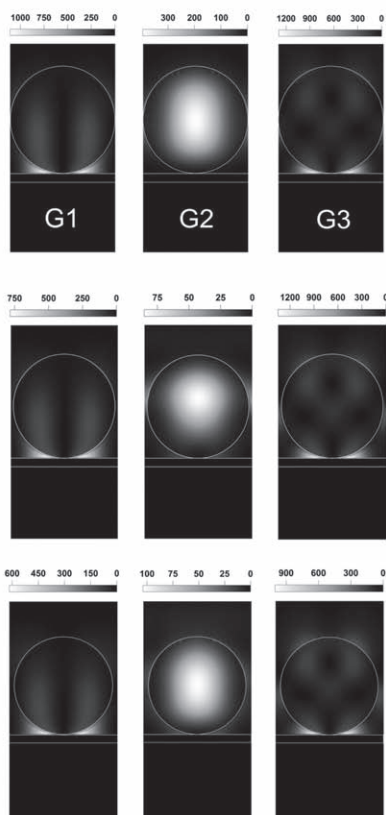
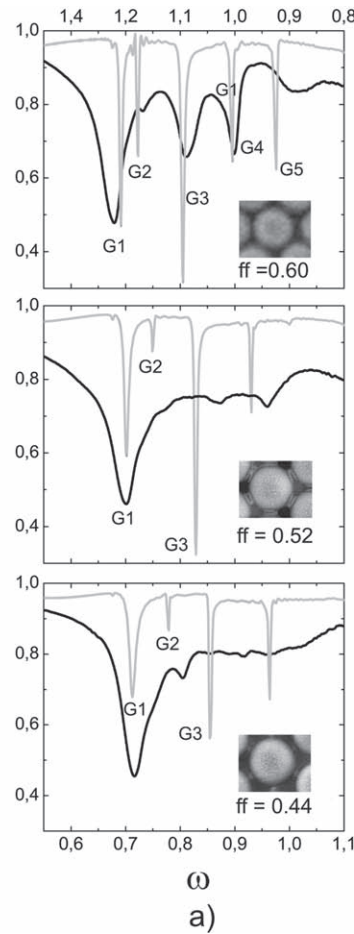


Figure 2. a) Normal incidence reflectance for three different filling fractions. Top to bottom: $ff = 0.6$, $ff = 0.52$, and $ff = 0.44$, corresponding to $\gamma = 1.0$, $\gamma = 0.95$, and $\gamma = 0.9$ respectively. Experimental (black) and theoretical spectra (grey) are presented. b) Total field intensity distribution and its evolution with sphere resizing for the first three modes in the left panel.

spectra where collected for a monolayer of $\phi = 1 \mu\text{m}$ spheres from the close-packed lattice until a 100 nm diameter reduction ($\gamma = 0.9$).

Figure 2 shows both experiment and simulated far-field reflectance for three different sphere diameters. As explained before,^[9,12,15] this kind of system supports hybrid modes along with the plasmonic resonances (SPP modes) provided by the metallic film and the photonic modes (WG modes) provided by the periodic structure of the monolayer of dielectric spheres. The five large dips shown in the reflectance spectra correspond to the modes of the sample. Coupling efficiency as well as field enhancement are dependent on the nature of each mode. For this study we will consider the first three modes (G1 to G3), representative of the three types of modes sustained by these systems, although the same behavior is obtained for the other two modes available (G4 and G5).

A good overall agreement between simulations and experimental data is found. However, some differences in spectral width and peak position is observed, most likely due to residual disorder introduced during the growth process. Polydispersity of the spheres can also be a source of defects, though in our

case its effect should not be significant due to the low values for the spheres used (less than 3% according to the manufacturer).

In order to characterize the modal distribution of the system, the total field intensity spatial distribution in the sample was numerically obtained. Figure 2b shows simulations where the structure is illuminated at normal incidence at those frequencies matching the G1, G2 and G3 modes. For the maximum filling fraction ($\gamma = 1$ or $ff = 0.6$), G1 and G3 show SPP-like character with a large field enhancement at the gold film surface, the main difference between the two modes being the field pattern within the sphere. For the G2 mode the field intensity remains mainly concentrated inside the spheres, indicating a WG-like nature. When $\gamma = 0.95$ ($ff = 0.52$) is achieved, all modes are blue-shifted. This is a consequence of the reduction in the effective refractive index of the dielectric region over the gold film as the spheres' volume fraction is reduced. On the one hand, SPR propagation is strongly dependent on the dielectric constant of the surrounding medium^[1] so a reduction of the effective refractive index of the metallic film loading material will spectrally shift SPRs to higher energies. On the other hand, the WG-like mode profile is determined by the size and shape of the spheres both of which dramatically change when the filling fraction of the total lattice is reduced.^[13,24] If we examine the total field distribution of the different modes as the filling fraction is reduced we can see that the WG and SP characters of the modes remain unchanged and only a slight decrease of the field is observed.

While results for only three etching steps have been shown above, the procedure can be carried out in a continuous manner allowing a fine degree of control of the sample topology and hence its optical response. To show this, reflectance spectra were recorded after each 30 second etching step over a 12.5 minute period corresponding to the first linear reduction region shown in Figure 1. As a result, $\phi = 1 \mu\text{m}$ spheres were reduced by as much as 100 nm in diameter ($0.44 < ff < 0.60$). Theoretical spectra like those in Figure 2 were calculated for each of the experimentally reduced diameters. For the experimental case, an initial diameter of $\phi = 1020 \text{ nm}$ was required in order to match the theoretical spectra, probably a consequence of the 3% polydispersity of the spheres. Nevertheless, the filling fraction reduction was comparable in both cases. The two reflectance maps obtained for simulations and experiments are plotted in Figure 3.

Figure 3a shows that as the filling fraction of the sample is reduced, the optical response undergoes two major changes. There is an overall blue-shift of the modes attributed, as already discussed, to a decrease in the effective index of the dielectric part of the system. There is also a change in the intensity of the

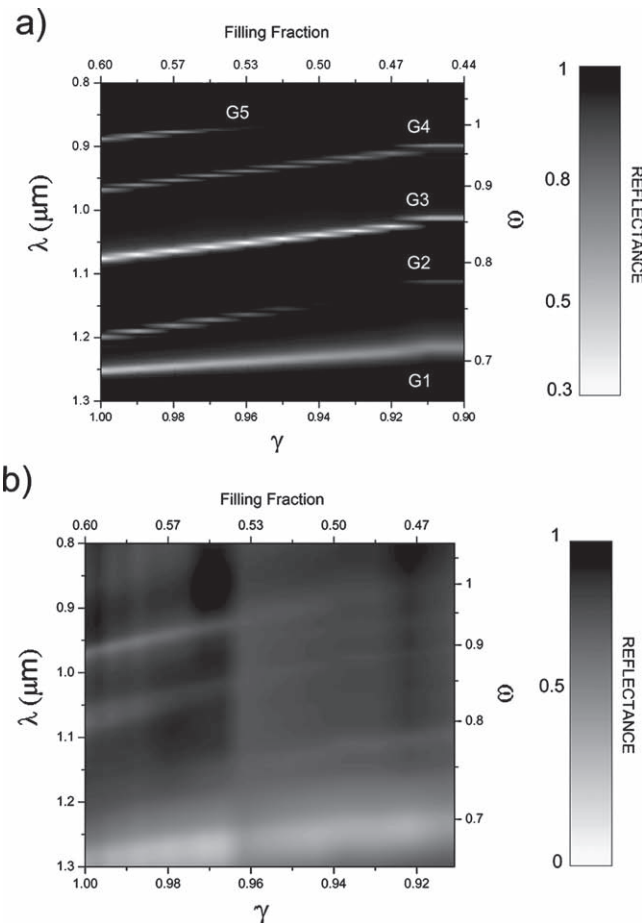


Figure 3. Calculated (a) and experimental (b) reflectance spectra represented as a contour plot for a monolayer of $\phi = 1 \mu\text{m}$ spheres as the filling fraction is varied from the close-packed lattice ($ff = 0.6$) to one with a 100 nm reduction in diameter ($ff = 0.44$).

dips in the reflectance spectra. While those modes that have a marked SP character (G1, G3) hardly change, those with a WG or hybrid character (G2, G4 and G5) present strong variations in intensity. This indicates that for the latter modes, when we reduce the sphere diameter, the spatial distribution of the field undergoes strong changes as already seen in the mode profiles of Figure 2. A clear example is the case of G2, where for $\gamma = 0.94$ the associated dip all but vanishes and then recovers upon further reduction. Accompanying this result is the increase of ca. an order of magnitude in the field intensity inside the spheres (see Figure 2).

When measurements are compared with calculations a good agreement is found. Modes G1, G3 and G4 present an identical linear blue-shift with ff reduction in both cases. Some differences are observed for experimental mode positions at ff below 0.5. This is due to the fact that the plasma reduction rate becomes slightly higher as the spheres are reduced. For the close-packed structure, G2 can hardly be appreciated due to the proximity of G1 which presents a very broad and intense dip, hiding the real value for reflectance at $\omega = 0.71$. However, it is possible to see that for $ff = 0.47$ ($\gamma = 0.92$) the coupling efficiency rises as was expected from theoretical results.

As a last analysis of mode evolution, it is observed in Figure 3a that the spectral shift of the resonances is linear with sphere diameter reduction. This fact is useful from the point of view of tuning several systems fabricated from the same initial spheres. Once the ratio has been estimated for one sample we can use optical characterization as a means to control the tuning of the optical response of the rest without recourse to SEM inspection,^[25] thereby making the process of tuning the optical features faster. Furthermore, the etching rates obtained could be slowed down or sped up depending on the conditions of the plasma process.

So far we have considered the tunability of the optical response of optically passive samples with the diameter of the spheres. The same tuning strategy has been adopted to modify the emission properties of a similar sample with luminescent properties (an optically active sample). In this case we have used Rhodamine 6G dye-doped $\phi = 520 \text{ nm}$ spheres. This diameter was chosen in order to overlap the dye's broad band emission spectrum with the G2 and G3 modes of the pristine sphere structure. Close-packed samples were subjected to an etching process for up to 7.5 min (corresponding to $\gamma = 0.88$ or a final $ff = 0.41$). Etching times were chosen in order to restrict the investigation to the linear reduction-rate region, as in the $\phi = 1 \mu\text{m}$ case. Figure 4 shows normal incidence reflectance and emission spectra for three different steps of the etching process. The close-packed structure shows the same modes as the $\phi = 1 \mu\text{m}$ sample, only not so well defined. This is due to the proximity of the optical features to the absorbance region of the gold film. Indeed, some difference in spectral mode position may exist due to the strong dispersion of gold in the new spectral range under study. Despite that, numerical simulations (not shown) demonstrate that the conclusions about modal evolution for the larger sphere samples are still valid in this case.

Emission for disordered dye-doped spheres (no photonic plasmonic effect) presents its maximum at 610 nm with 70 nm spectral width. When the spheres are in a close-packed lattice, emission can be strongly enhanced for those frequencies spectrally matching a mode of the structure.^[9] In particular the WG-like mode (G2) is the most suitable to enhance the dye's emission given that its field profile matches the geometrical position of the dye molecules in the structure (inside the sphere). Figure 4a (close-packed sample, $ff = 0.6$) shows the strong emission enhancement taking place for $\omega = 0.71$, corresponding to the G2 mode. Emission enhancement for $ff = 0.6$ also takes place at $0.73 < \omega < 0.78$, associated with mode G3. For G1 no enhancement exists due to the fact that it is spectrally far from the emission of the dye.

When the diameter of the spheres is reduced under plasma etching the blue-shift of the modes in reflectance, already studied for the $\phi = 1 \mu\text{m}$ case, is now only observed in the visible spectral range. Upon comparison of reflectance and emission spectra (Figure 4) it is evident that the peaks of enhanced emission follow the trend of dips in reflectance, corresponding to the modes of the structure. In this way one can effectively tune the sample's emission by controlling the plasma process. Beside the spectral shift, changes in the magnitude of emission enhancement taking place as the etching process advances are a combination of two factors. The first can be associated with the variations in the field confinement taking place as we reduce

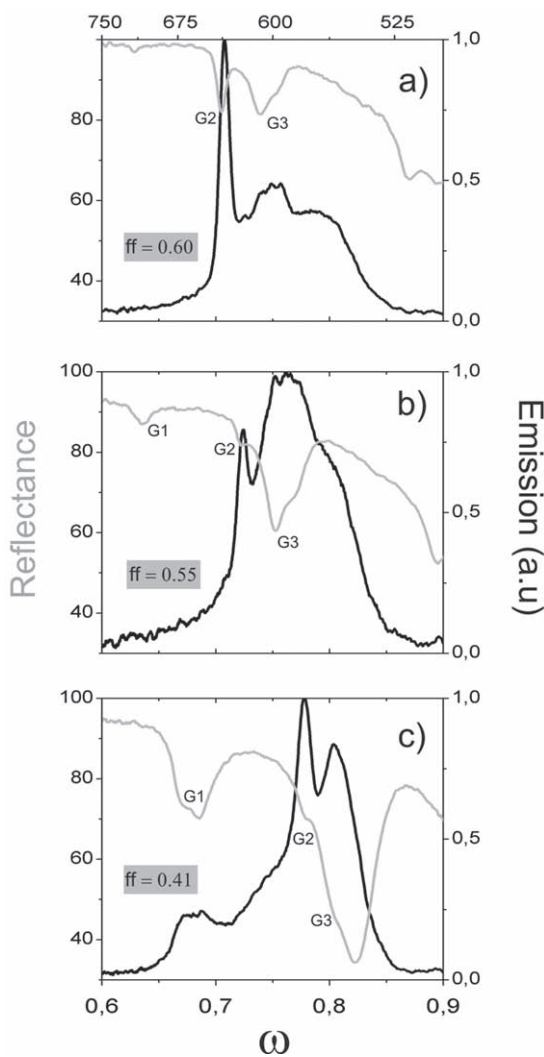


Figure 4. Normal incidence reflectance (grey) and emission (black) spectra for $\phi = 520$ nm dye-doped spheres at three different filling fractions corresponding to $\gamma = 1$ (a), $\gamma = 0.97$ (b), and $\gamma = 0.88$ (c).

the sphere diameter (see discussion above and Figure 2) and the second to the fact that, as the reduction process takes place, the modes of the system are swiped across the dye's broad emission so that enhanced emission should be more probable the closer a mode is to the dye's emission maximum.

A clear example of the above is that of mode G1, of SPP-like character. While for $ff = 0.6$ (Figure 4a) no enhanced emission takes place at the spectral position of this mode ($\omega = 0.62$) owing to the fact that it is far from the dye's emission, as we decrease the sphere diameter we shift its spectral position until for $\gamma = 0.95$ it eventually overlaps the dye's emission ($ff \approx 0.51$). At that point, emission enhancement is already visible; moreover it is clear that as γ reduces and the mode blue-shifts, the emission increases as can be seen for $ff = 0.41$ and $\omega = 0.68$ in Figure 4c. The fact that such enhancement is not as large as for the other modes is due to the small spatial overlap between the dye and the field, mainly concentrated near the gold surface. Finally it must be noted that as the etching process takes place the effects

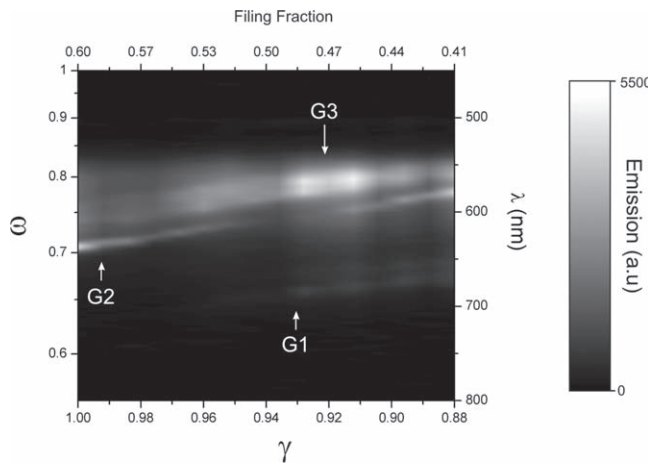


Figure 5. Emission (in arbitrary units) as a contour plot for a monolayer of $\phi = 520$ nm dye-doped PS spheres in a continuous filling fraction reduction process. Oxygen-plasma etching was carried out from the close-packed scenario ($ff = 0.60$) to a final filling fraction of $ff = 0.41$.

of disorder, broadening the peaks in reflectance, become more evident. This is likely responsible for the discrepancy between reflectance and emission of the G3 peak in the case of the smallest filling fraction (Figure 4c). Here the reflectance peak broadens considerably, causing a part of the peak to fall in the high energy tail of the emission (where it is less efficient) and hence causing an asymmetry of the emission peak.

As was done for the $\phi = 1\text{ }\mu\text{m}$ spheres with reflectance measurements, a map of the emission of the $\phi = 520$ nm spheres has been created as the sphere size is reduced in small steps (Figure 5). Here several facts are worth mentioning. Firstly, we can trace the evolution of mode G2 and see that as we reduce the sphere diameter we can not only continuously shift its spectral position but also modulate its intensity, taking it to a minimum for $\gamma \approx 0.94$ ($ff = 0.49$). For even larger diameter reductions we see how it recovers its intensity. The SPP-like G1 mode now appears as an enhancement in emission for $\gamma \sim 0.95$, as we shift it towards the dye's emission. Finally mode G3 is also seen to blue-shift and reach a maximum as it overlaps the highest value of the dye's emission for $ff = 0.47$. Nevertheless, the behavior observed in the emission for the $\phi = 520$ nm qualitatively matches that of the observed reflectance for the $\phi = 1\text{ }\mu\text{m}$ sample, indicating that although we are considering different spectral regions, where the dielectric constant of gold changes, the system still presents acceptable scalability.

3. Conclusion

In conclusion, we have shown a straightforward method to fine-tune the plasmonic-photonic hybrid modes of one monolayer of PS spheres deposited on a gold substrate. It has been demonstrated that a small reduction of filling fraction of the lattice produces large spectral blue-shifts as well as variations on the spatial distribution of the total field intensity depending on the character (SPP-like or WG-like) of the mode studied. These changes are accompanied by a strong modification of the sample's optical response both in reflectance and emission when

optically active spheres are used. Experimental results have been numerically modeled and a good agreement was found, which is remarkable since modal distribution has been found to be very sensitive to small changes in the structure's morphology. The easy and inexpensive method to finely tune the optical properties of the samples could find application in some active research fields such as organic emitting devices. Further, since the magnitude of the structural changes we have imposed on our samples are similar to those achievable with tunable polymeric spheres made from hydrogels, these results could be applied as a proof of principle for future sensing devices where tunability is achieved by means of external stimuli.

4. Experimental Section

Sample Fabrication: Close-packed monolayers were fabricated by the vertical deposition method.^[29] A rigid substrate was introduced vertically in a colloidal suspension with a controlled concentration (0.08% wt.) low enough to produce a layer just one sphere thick. The growth was performed in an oven under stabilized temperature (50 °C) and humidity (20%). We used commercial PS spheres (Duke Scientific) with two different diameters: 0.52 and 1 μm. The former spheres had an organic dye (Rhodamine 6G) homogeneously distributed throughout their volume. Their diameter was chosen to tune optical features to the appropriate spectral range in each case. The $\phi = 1 \mu\text{m}$ spheres were chosen to tune the lowest energy mode (G1) to the NIR range and allow us to place as many higher-energy modes as possible in the VIS-NIR range which is where the optical detectors we used (Si/InSb) perform best. One should take into account that, when working at these wavelengths, large negative real values of the dielectric constant of gold provide the best performance when SPP modes are considered. On the other hand, for $\phi = 520 \text{ nm}$, the condition was to overlap the G1 to G4 modes with the dye's emission spectrum. As a substrate, we used 450 μm thick silicon wafers (ACM) on which a thin (60 nm) gold film was sputtered.

For sphere reduction a commercial oxygen-plasma etching stripper (Tetra Pico from Diener Electronics) was used. The exposure time was controllable with a minimum etching step of 10 seconds.

Optical Measurements: To optically characterize the sample two different set-ups were used. For normal incidence reflectance measurements in the NIR spectral range we used a Fourier Transform Infrared (FTIR) spectrometer coupled to a 4x microscope objective with a low Numerical Aperture (NA = 0.1). For reflectance/emission spectra at visible wavelengths we used a large numerical aperture (NA = 0.75) 40x microscope objective coupled to a microscope. Its output was collected by a 100 μm core optical fiber coupled to a portable spectrometer (Ocean Optics 2000+ USB).

Simulations: Numerical simulations were performed with commercial software (Lumerical FDTD Solutions) from which normal incidence reflectance spectra were calculated along with the spatial distribution of the total field intensity at those wavelengths where mode excitation takes place. The presence of the gold layer, together with the possible coupling to localized excitations makes it necessary to employ a fine grid (40 points per wavelength in each direction) as well as long enough simulation time.

Acknowledgements

The authors would like to acknowledge Jorge Sánchez-Marcos for providing high quality gold coated substrates. J.F. G-L was supported by the JAE Postdoctoral Program from the CSIC. M. L-G was supported by the FPI PhD program from the MICINN. This work was partially supported by EU FP7 NoE Nanophotonics4Energy grant No. 248855; the Spanish MICINN CSD2007-0046 (Nanolight.es), MAT2009-07841 (GLUSFA),

CSIC PIF08-016 (Intramural Frontera) and Comunidad de Madrid S2009/MAT-1756 (PHAMA) projects. A. García-Martín also acknowledges financial support from the Spanish MICINN ("MAGPLAS" MAT2008-06765-C02-01/NAN, Funcoat Consolider Ingenio 2010 CSD2008-00023) and European Comission (NMP3-SL-2008-214107-Nanomagma).

Received: June 11, 2010

Revised: July 26, 2010

Published online: October 5, 2010

- [1] W. L. Barnes, A. Dereux, T. W. Ebbesen, *Nature* **2003**, *424*, 824.
- [2] A. Blanco, E. Chomski, S. Grabczak, M. Ibáñez, S. John, S. W. Leonard, C. Lopez, F. Meseguer, H. Miguez, J. P. Mondia, G. A. Ozin, O. Toader, H. M. van Driel, *Nature* **2000**, *405*, 437.
- [3] M. Fujita, S. Takahashi, Y. Tanaka, T. Asano, S. Noda, *Science* **2005**, *308*, 1296.
- [4] P. Lodahl, A. F. van Driel, I. S. Nikolaev, A. Irman, K. Overgaag, D. L. Vanmaekelbergh, W. Vos, *Nature* **2004**, *430*, 654.
- [5] R. F. Oulton, V. J. Sorger, T. Zentgraf, R.-M. Ma, C. Gladden, L. Dai, G. Bartal, X. Zhang, *Nature* **2009**, *461*, 629.
- [6] J. Grandidier, S. Massenot, G. Colas des Francs, A. Bouhelier, J. C. Weeber, L. Markey, A. Dereux, J. Renger, M. U. Gonzalez, R. Quidant, *Phys. Rev. B* **2008**, *78*, 245419.
- [7] T. A. Kelf, Y. Sugawara, J. J. Baumberg, M. Abdelsalam, P. N. Bartlett, *Phys. Rev. Lett.* **2005**, *95*, 116802.
- [8] G. Vecchi, V. Giannini, J.G. Rivas, *Phys. Rev. Lett.* **2009**, *102*, 146807.
- [9] M. López-García, J. F. Galisteo-López, A. Blanco, J. Sánchez-Marcos, C. López, A. García-Martín, *Small* **2010**, *6*, 1757.
- [10] J. Sun, C. Tang, P. Zhan, Z. Han, A. Cao, Z. Wang, *Langmuir* **2010**, *26*, 7859.
- [11] Y. Li, W. Cai, G. Duan, *Chem. Mater.* **2007**, *20*, 615.
- [12] R. M. Cole, J. J. Baumberg, F. J. García de Abajo, S. Mahajan, M. Abdelsalam, P. N. Bartlett, *Nano Lett.* **2007**, *7*, 2094.
- [13] H. Miyazaki, K. Ohtaka, *Phys. Rev. B* **1998**, *58*, 6920.
- [14] R. M. Cole, Y. Sugawara, J. J. Baumberg, S. Mahajan, M. E. Abdelsalam, P. Bartlett, *Phys. Rev. Lett.* **2006**, *97*, 137401.
- [15] L. Shi, X. Liu, H. Yin, J. Zi, *Phys. Lett. A* **2009**, *374*, 1059.
- [16] X. Yu, L. Shi, D. Han, J. Zi, P. V. Braun, *Adv. Funct. Mater.* **2010**, *20*, 1910.
- [17] L. Landström, D. Brodoceanu, D. Bäuerle, F. J. García-Vidal, S. G. Rodrigo, L. Martin-Moreno, *Opt. Express* **2009**, *17*, 761.
- [18] D. Pacifici, J. Henri, H. A. Atwater, *Nat. Photonics* **2007**, *1*, 402.
- [19] P. R. Evans, G. A. Wurtz, W. R. Hendren, R. Atkinson, W. Dickson, A. V. Zayats, R. J. Pollard, *Appl. Phys. Lett.* **2007**, *91*, 043101.
- [20] V. V. Temnov, G. Armelles, U. Woggon, D. Guzatov, A. Cebollada, A. García-Martín, J. M. García-Martín, T. Thomay, A. Leitenstorfer, R. Bratschitsch, *Nat. Photonics* **2010**, *4*, 107.
- [21] J. B. González-Díaz, A. García-Martín, G. Armelles, J. M. García-Martín, C. Clavero, A. Cebollada, R. A. Lukaszew, J. R. Skuza, D. P. Kumah, R. Clarke, *Phys. Rev. B* **2007**, *76*, 153402.
- [22] D. Gérard, V. Laude, B. Sadani, A. Khelif, D. Van Labeke, B. Guizal, *Phys. Rev. B* **2007**, *76*, 235427.
- [23] S. Furumi, H. Fudouzi, T. Sawada, *Laser Photon. Rev.* **2009**, *4*, 205.
- [24] T. Fujimura, T. Tamura, T. Itoh, C. Haginoya, Y. Komori, T. Koda, *App. Phys. Lett.* **2001**, *78*, 1478.
- [25] A. Plettl, F. Enderle, M. Saitner, Achim Manzke, C. Pfahler, S. Wiedemann, P. Ziermann, *Adv. Funct. Mater.* **2009**, *19*, 3279.
- [26] G. von Freymann, S. John, V. Kitaev, G. A. Ozin, *Adv. Mater.* **2005**, *17*, 1273.
- [27] T. Ding, K. Song, K. Clays, C.-H. Tung, *Langmuir* **2010**, *26*, 4535.
- [28] C. Haginoya, M. Ishibashi, K. Koike, *App. Phys. Lett.*, **1997**, *71*, 2934.
- [29] P. Jiang, J. F. Bertone, K. S. Hwang, V. L. Colvin, *Chem. Mater.* **1999**, *11*, 2132.